

Spatially direct and indirect photoluminescence from InAs/AlSb heterostructures

F. Fuchs, J. Schmitz, J. D. Ralston, and P. Koidl

Fraunhofer Institut für Angewandte Festkörperphysik, Tullastrasse 72, D-79108 Freiburg, Federal Republic of Germany

(Received 6 December 1993)

We present a Fourier-transform photoluminescence study of InAs/AlSb type-II heterostructures, spanning the midinfrared 1–12- μm wavelength range. The investigated samples consist of single and double quantum wells, grown on GaAs substrates by molecular-beam epitaxy, with different buffer-layer structures for strain accommodation. The photoluminescence intensity is found to be very sensitive to the detailed structure of the underlying buffer sequence. The use of a GaSb buffer or a GaSb/AlSb superlattice in the buffer gives rise to an additional radiative-recombination channel in the near infrared, which competes with radiative recombination in the InAs quantum wells at longer wavelengths. Variations in the spectra observed under visible and infrared excitation provide evidence that the recently observed persistent photo effect is governed by hole capture in the GaSb layers in the buffer sequence. Furthermore, very wide quantum wells (100 and 200 nm) show spatially direct as well as spatially indirect photoluminescence, providing insight into the nature of the transition from the bulklike semiconductor to the type-II heterostructure.

I. INTRODUCTION

Heterostructures based on the InAs/AlSb/GaSb material system are attracting increasing interest because of their very promising technological applications¹ and unique physical properties. The valence-band maximum of the AlSb barrier is about 100 meV above the valence-band maximum of InAs, whereas the conduction-band minimum resides in the InAs layers. The conduction-band offset² has a value of 1.35 eV in the case of the indirect band gap and 1.95 eV at the Γ point, providing excellent electronic confinement (see inset in Fig. 1). This type-II band alignment leads to a spatial separation of electrons and holes. The very large conduction-band offset is of the order of the energy barrier between the semiconductor and the vacuum. Therefore, Tamm states,³ which are associated with the heterointerface, may be important for the understanding of the properties of the InAs/AlSb interface, which can be driven via the epitaxial growth sequence to be AlAs- or InSb-like. A further important question under discussion with respect to the existence of Tamm states is the origin of part of the very high electron concentrations³ (typically on the order of 10^{12} cm^{-2}). They are found in InAs/AlSb quantum wells even in the absence of intentional doping, with mobilities⁴ routinely exceeding $10^5 \text{ cm}^2/\text{V s}$. This high concentration is partly attributed to a surface contribution^{5,6} in the case of small AlSb barriers between the InAs well and the GaSb cap layer. The main contribution is shown⁷ to originate from the AlSb barrier material. Recently, it has been suggested⁸ that the cation-on-anion antisite defect establishes a deep level in the AlSb barrier, which should be responsible for the dominant contribution of the observed remote doping of the InAs channels.

In contrast to the intense investigation of the transport properties of the above material system¹ there have been very few reports on the optical properties. Besides far-

infrared magneto-optical transport studies,^{9,10} there have been published Raman investigations focusing on heterostructure interface properties.^{11–13} Photoluminescence (PL) in the near infrared on *narrow* InAs/AlSb superlattices (SL's) has also been reported.¹⁴ Recently, we have presented a study of the midinfrared emission of *wide* single quantum wells (SQW's),¹⁵ with the optical data showing good correlation to the measured transport proper-

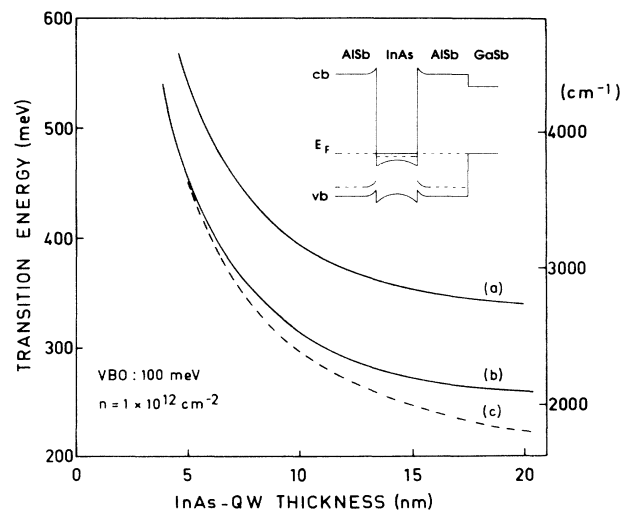


FIG. 1. Self-consistent two-band calculation of the dependence of the transition energy of InAs/AlSb type-II heterostructures on the QW width, assuming a valence-band offset (VBO) of 100 meV as indicated in the inset. The biaxial tensile strain due to relaxation of the AlSb layer (b) leads to a reduction of the band gap to 287 meV and an effective mass of $0.0187m_0$. Growth on GaSb (a) leads to a higher band gap of 357 meV and higher effective mass. In (a) and (b) an electron sheet density of $n = 1 \times 10^{12} \text{ cm}^{-2}$ was assumed, which affects the wider QW's. Neglecting the space-charge effects (depopulated wells) results in the well-width dependence shown in (c).

ties. In Ref. 15 the persistent photo effect^{16,17} could be observed by PL, where a broadening and blueshifting of the spectra was observed in the case of long-wavelength excitation. This was explained by a photo-induced enhancement of the electron concentration raising the Fermi energy to a maximum value limited by an apparent resonance with a defect-related deep level^{8,7} 400 meV above the valence-band maximum of the AlSb barriers. Following Shen *et al.*⁸ we have attributed this level to the AlSb antisite.

In the present work, a detailed analysis of the influence of the epitaxial buffer-layer sequence on the PL intensity will be presented. It will be shown that the PL intensity, as well as the persistent photo effect, is governed by hole capture. Because of the valence-band alignment, the GaSb layers act as a sink for the photo-generated holes, preventing them from recombining with the electrons confined in the InAs QW's (see inset in Fig. 1). Furthermore, very wide quantum wells were investigated (100 and 200 nm). These wide quantum wells show both the spatially *direct* transitions of the InAs well and the spatially *indirect* radiative recombination of electrons and holes across the type-II heterointerface. This behavior provides further insight into the transition from a bulk-like semiconductor to a type-II heterostructure.

II. EXPERIMENTAL

The samples were grown by solid-source molecular-beam epitaxy (MBE) on (100) GaAs substrates. The arsenic flux was controlled by a valved-cracker effusion cell, which facilitates the reduction of the arsenic background pressure during growth by up to three orders of magnitude as compared to conventional arsenic effusion cells.¹⁸ As has been demonstrated in Refs. 18 and 19, MBE growth of binary AlSb layers with a *conventional* cell leads to the formation of ternary AlAs_{1-x}Sb_x alloys with arsenic mole fractions typically exceeding 10%. The structures investigated here consist of a 100-nm GaAs buffer followed by two periods of a 4-ML AlAs–2-ML GaAs short-period superlattice with a 100-nm AlSb nucleation layer on top. Next, a thick (1000 nm) relaxed AlSb or GaSb buffer was grown for accommodation of the lattice-constant misfit. One sample also had a GaSb/AlSb short-period SL grown on the AlSb buffer. The InAs/AlSb QW structure was deposited with a 40-nm AlSb barrier below and a 10-nm barrier on top. The shutter sequence was programmed so as to promote InSb-like interfaces,⁴ which was confirmed following the MBE growth via Raman measurements.^{13,18} Finally, the structures were capped with 10 nm of GaSb to prevent degradation.

The optical measurements were carried out with a Fourier-transform spectrometer, using double-modulation techniques as described elsewhere.²⁰ An InSb photodiode operating at 77 K was used to detect the PL. The samples were positioned in a He exchange gas cryostat. Optical excitation was accomplished either with visible radiation from an argon laser (2.54 or 2.71 eV) or with the ir radiation of a YAG:Nd laser (where YAG is yttrium aluminum garnet) (0.94 or 1.17 eV).

III. RESULTS AND DISCUSSION

The calculated dependence of the PL transition energy on the QW width, using a self-consistent two-band model, is shown in Fig. 1. Due to growth on a strain-relaxed GaSb (a) or AlSb buffer (b), biaxial tensile strain decreases the band gap¹⁰ of InAs to a value of 357 or 287 meV, respectively. In (a) and (b) an electron concentration of $1 \times 10^{12} \text{ cm}^{-2}$ has been assumed. If the electrostatic band bending is neglected (i.e., undoped QW's), significant deviation occurs for the wide QW's, as shown by curve (c) in Fig. 1. To obtain the transition energies of the spatially indirect PL a valence-band offset of 100 meV between InAs and AlSb has been assumed.

The PL intensity is found to be very sensitive to the structure of the buffer sequence, as shown in Fig. 2. Spectrum (a) has been obtained from a 5-nm InAs SQW grown on a GaSb/AlSb short-period SL on top of AlSb buffer. Spectrum (b) corresponds to a 7.5-nm SQW grown on top of a GaSb buffer. Spectrum (c) is observed from a double quantum well (DQW), where the two 7.5-nm InAs channels were separated by an AlSb barrier of 7.5 nm width. Spectrum (d) has been obtained from a 7.5-nm InAs DQW sample grown on an AlSb buffer with no GaSb layers inserted. The spectra are corrected for the system response and scaling factors are indicated in the figure.

In Fig. 2 we observe a strong anticorrelation of the PL intensity of the InAs quantum-well structure with the PL intensity of the buffer layers. Strong radiative recombination from the short-period SL is observed in the near ir spectrum (a), where the intensity of the InAs SQW is very

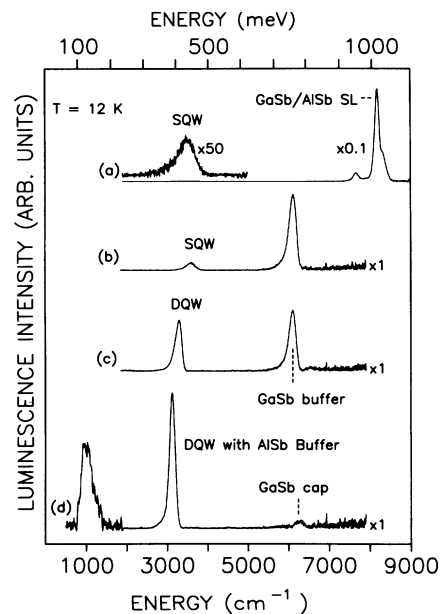


FIG. 2. Evolution of the PL intensity with change of the buffer structure (a) 5-nm single quantum well grown with a GaSb/AlSb short-period SL on top of an AlSb buffer, (b) 7.5-nm SQW with a GaSb buffer, (c) 7.5-nm double quantum well with a GaSb buffer, (d) 7.5-nm DQW with an AlSb buffer, using GaSb only for the cap layer. The spectra are corrected for the system response.

weak. In contrast, the DQW structure grown on a thick AlSb buffer (d), which does not show PL in the near ir, exhibits very strong emission from the InAs QW's. The intensity variation of the QW emission covers about two orders of magnitude. It is interesting to note that the sample with the most intense PL (d) exhibits an additional transition around $10 \mu\text{m}$, which is comparable to the intensity of the QW emission. The cutoff at 650 cm^{-1} of this spectrum is given by the $\text{Hg}_{1-x}\text{Cd}_x\text{Te}$ photoconductor which has been used for detection of the low-energy part. We will discuss this low-energy transition in the framework of Tamm states later. In the following we concentrate on the intensity dependence of spectra (a)–(d).

A. Hole generation, diffusion, and trapping

From the spectra shown in Fig. 2 it is evident that GaSb layers in the buffer sequence introduce a competing recombination channel, due to the type-II band alignment of the materials (see inset in Fig. 1). Only sharp interfaces provide finite spatial overlap of the electron and hole wave functions, to enable radiative recombination involving the InAs QW's. Due to electrostatic band bending there is some localization of the hole at the heterointerfaces. However, the photo-generated holes can relax energetically into the GaSb layers, where the valence band is located about 0.35 eV above the valence-band maximum of AlSb.^{2,17} This is confirmed by the intensity enhancement by a factor of 5 observed with a DQW compared to a SQW, where the hole confinement between the two InAs channels prevents diffusion away from the heterointerfaces. Finally, the most intense PL is observed from the sample containing no GaSb layers (d).

The above explanation is further supported by the results of measurements on a sample containing three InAs single quantum wells grown on top of an AlSb buffer layer (Fig. 3). The narrowest QW (5 nm) was grown first, followed by a 10-nm QW, with the widest QW (20 nm) located closest to the sample surface. The QW's were separated by 7.5-nm AlSb barriers, such that coupling of the electron wave functions is not significant. The expected transition energies according to Fig. 1 are indicated with vertical dashed lines. We observe two lines, where the spectral shape of the low-energy transition is altered when the excitation wavelength is changed. This is caused by the overlap of the emission of the two wider QW's which will be shown later.

First, we concentrate on the evolution of the *relative* intensities while changing the excitation from the ir [Fig. 3(a)] to the visible [Figs. 3(b) and 3(c)]. Despite the shorter penetration length of the visible excitation, the relative intensity of the 5-nm QW increases in the case of 2.71-eV excitation. The ir excitation, which is only absorbed by the InAs QW's, leads to a relative enhancement of the PL from the wider QW's located above.

In the case of visible excitation, the hole generation takes place predominantly in the AlSb buffer, resulting in the relative enhancement of the intensity of the 5-nm SQW. This is because this QW is located closest to the AlSb buffer. The ir excitation, however, cannot be ab-

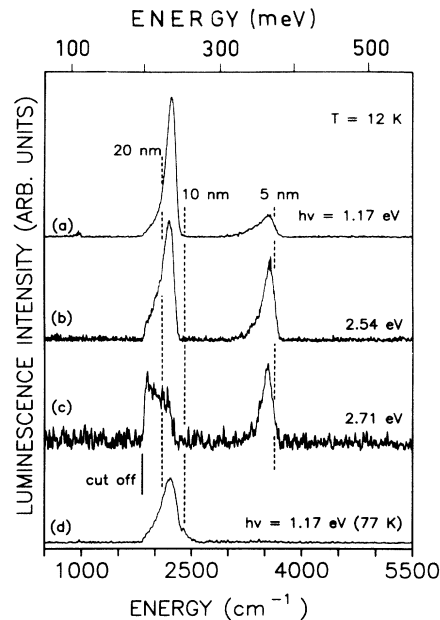


FIG. 3. PL of three InAs single quantum wells (5, 10, and 20 nm width) embedded in an AlSb matrix. The dependence on photon energy of the excitation is shown. The transitions of the two wider quantum wells overlap, due to the increase of the transition energy of the 20-nm QW (populated).

sorbed by the AlSb buffer, and the hole generation then takes place exclusively at the InAs QW. In the present structure the photo-generated holes are then confined in the AlSb barriers between the three InAs QW's. The 10-nm QW in the middle of the heterostructure is confined by two AlSb barriers and in the case of ir excitation the 10-nm QW indeed exhibits the most intense emission.

The above explanation accounts for the observation of only two separate lines in Fig. 3, while the structure consists of three QW's. The emission of the 20-nm QW will be weaker in intensity as compared to the 10-nm QW. Moreover, according to Fig. 1, the transition of the 20-nm QW is expected to shift to higher energies due to the high electron concentration, resulting in an overlap with the transition of the 10-nm QW, which is depopulated. For these two reasons we only observe a change in spectral shape when changing the excitation wavelength.

An increase of the sample temperature to 77 K [spectrum (d) in Fig. 3] provides further support for the picture outlined above. The emission of the 5-nm QW disappears, while the PL of the two other QW's remains detectable. Thus, at higher temperature the holes located at the lowest heterointerface of the 5-nm QW diffuse away toward the substrate, while the confined holes still give rise to PL from the 10- and 20-nm QW's.

These results also give insight into the persistent photo effect,^{16,17} which has recently been observed in similar structures. Samples which contain GaSb layers in the buffer structure showed a strong blueshifting and broadening of the PL spectra in the case of ir excitation.¹⁵ This was explained by an increase of the electron concentration in the InAs channels. The present results

reveal that this enhancement in electron concentration is made possible by hole capture in the GaSb layers in the buffer sequence. Consequently, the heterostructures grown here without GaSb layers in the buffer do not show a significant change of the spectral shape when the excitation energy is changed, because there is no spatial separation of the photo-generated holes away from the QW interfaces. The PL results presented above can thus be consistently understood in terms of hole generation, diffusion, and capture, which are all strongly influenced by the presence of GaSb layers in the buffer sequence.

B. Tamm states

We now focus on the emission at a transition energy around 100 meV (10 μm) shown in spectrum (d) of Fig. 2, which was observed from the 7.5-nm-wide DQW under ir illumination. It is quite surprising to observe such an intense emission in this spectral region. This emission is observed only under ir excitation conditions, where the hole generation takes place exclusively in the InAs QW's. This opens the discussion whether Tamm states are responsible for this transition. As outlined by Kroemer and co-workers³ a simple approximation of the influence of these interface states is given by adding a δ -like potential spike at the interface. In the case of a hole-attracting potential spike, this could explain the localization of the holes at the interface which makes PL possible. This interpretation assigns the low-energy transition at 10 μm to the radiative recombination of the electrons in the InAs well with holes localized in the potential step associated with Tamm states of the heterointerface. However, further experiments must be carried out in order to confirm this hypothesis.

C. Spatially indirect and direct transitions

In this section, we consider very wide InAs layers with thicknesses of 100 and 200 nm sandwiched between 40-nm-thick AlSb barriers grown on a 1000-nm GaSb buffer layer. In such wide QW's we have to expect the formation of triangular-shaped electron channels at the top and bottom heterointerfaces, due to the electrostatic band bending. Furthermore, due to comparable dimensions of the layer thickness and hole diffusion length, this type of sample will also exhibit bulklike properties.

The spectra obtained from these two very wide InAs QW's are shown in Fig. 4. These samples do not exhibit any detectable signal at transition energies below 220 meV. Besides a weak feature at 250 meV, the spectrum of the 200-nm layer (bottom) consists of one single line. This line is located at an energy of 366 meV, in excellent agreement with the prediction of an InAs band gap¹⁰ of 357 meV in the case of biaxial tensile strain due to growth on GaSb. Comparing this spectrum with the emission of the 100-nm layer, only a weak transition is observed at about the same spectral position, while two broad bands at lower transition energy become dominant. These bands are separated from the transition at 366 meV by energies of 74 and 124 meV. The relative intensity of the two bands is altered when the excitation wave-

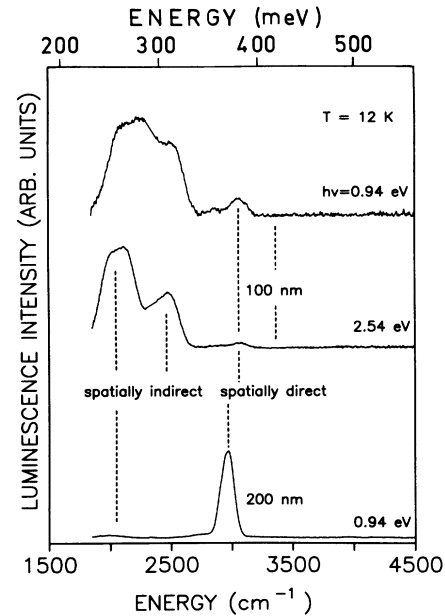


FIG. 4. Spatially direct and indirect PL of every wide InAs quantum wells.

length is changed. For visible excitation the high-energy component is enhanced, whereas the spectral shape of the individual components is not affected significantly.

Due to band bending in the 200-nm-wide layer, there will be a weak confinement attracting the photo-generated holes toward the center of the InAs layer (see inset in Fig. 1), thus preventing them from diffusing toward the AlSb layers. This explains the strong PL intensity at the energy expected for the bulk transition. Therefore, the high-energy transition at 366 meV is due to spatially *direct* recombination in the bulklike InAs layer. In the 100-nm layer the hole confinement is weakened, since the influence of band bending decreases with decreasing layer width. In addition the photo-generation of holes in the InAs layer itself is decreased due to the decrease in layer thickness. Thus, the spatially *indirect* transitions across the heterointerfaces become dominant.

We do not directly observe an energy difference of 100 meV between the direct and indirect PL peaks as expected from the value of the valence-band offset, because of electron confinement in the triangular-shaped potential wells at the two interfaces. Furthermore, as pointed out in Ref. 15, there is evidence for an acceptor level 80 meV above the AlSb valence-band maximum, which also leads to redshift of the PL transitions. The relative enhancement of the high-energy part of the indirect PL in the case of visible excitation indicates that this component originates from the lower interface, which contains a higher electron concentration than the top channel. This behavior is in full agreement with the previous results, which indicated that the excess holes are spatially separated in the GaSb buffer, which then leads to electron accumulation in the channel of the lower heterointerface.

IV. CONCLUSION

We have studied the photoluminescence of InAs/AlSb heterostructures and investigated in detail the influence of the buffer-layer sequence on the PL spectra. Samples which do not contain GaSb layers in the buffer sequence exhibit PL signals which are two orders of magnitude stronger than those from samples with GaSb layers in the buffer sequence. Generation, diffusion, and capture of the photo holes are all shown to influence both the PL intensity and the photo-induced change of the electron concentration. The relaxation of photo-generated holes into the underlying GaSb layers of the buffer system, leading to spatial separation of the excess carriers, is a key mechanism. The observation of a very intense emission in the spectral range around $10\ \mu\text{m}$ lends preliminary support

to the hypothesis that Tamm states might be relevant for the interface properties. The PL from very wide InAs layers provides insight into the transition from a type-II heterostructure to a bulk semiconductor, due to the observation of both spatially direct and spatially indirect radiative transitions.

ACKNOWLEDGMENTS

Helpful discussions with J. Wagner and the support of H. Schneider in performing the self-consistent calculations are gratefully acknowledged. The authors also thank K. Schwarz and G. Bihmann for expert technical assistance. This work was performed as part of the topical program "III-V Electronics" supported by the Bundesminister für Forschung und Technologie (BMFT).

-
- ¹A. G. Milnes and A. Y. Polyakov, *Mater. Sci. Eng. B* **18**, 237 (1993).
- ²A. Nakagawa, H. Kroemer, and J. H. English, *Appl. Phys. Lett.* **54**, 1893 (1989).
- ³H. Kroemer, C. Nguyen, and B. Brar, *J. Vac. Sci. Technol. B* **10**, 1769 (1992); H. Kroemer, *ibid.* **11**, 1354 (1993).
- ⁴G. Tuttle, H. Kroemer, and J. H. English, *J. Appl. Phys.* **67**, 3032 (1990).
- ⁵C. Nguyen, B. Brar, and H. Kroemer, *Appl. Phys. Lett.* **60**, 1854 (1992).
- ⁶C. Nguyen, B. Brar, and H. Kroemer, *J. Vac. Sci. Technol. B* **11**, 1706 (1993).
- ⁷S. Ideshita, A. Furukawa, Y. Mochizuki, and M. Mizuta, *Appl. Phys. Lett.* **60**, 2549 (1992).
- ⁸J. Shen, J. D. Dow, S. Y. Ren, S. Tehrani, and H. Goronkin, *J. Appl. Phys.* **73**, 8313 (1993).
- ⁹J. Scriba, S. Seitz, A. Wixforth, J. P. Kotthaus, G. Tuttle, J. H. English, and H. Kroemer, *Surf. Sci.* **267**, 483 (1992).
- ¹⁰M. J. Yang, P. J. Lin-Chung, R. J. Wagner, J. R. Waterman, W. J. Moore, and B. V. Shanabrook, *Semicond. Sci. Technol.* **8**, S129 (1993); M. J. Yang, P. J. Lin-Chung, B. V. Shanabrook, J. R. Waterman, R. J. Wagner, and W. J. Moore, *Phys. Rev. B* **47**, 1691 (1993).
- ¹¹Y. Iwai, M. Yano, R. Hagiwara, and M. Inoue, *Surf. Sci.* **267**, 434 (1991).
- ¹²I. Sela, C. R. Bolognesi, L. A. Samoska, and H. Kroemer, *Appl. Phys. Lett.* **60**, 3283 (1992).
- ¹³J. Wagner, J. Schmitz, J. D. Ralston, and P. Koidl, *Appl. Phys. Lett.* **64**, 82 (1994).
- ¹⁴B. Brar, H. Kroemer, J. Ibbetson, and J. H. English, *Appl. Phys. Lett.* **62**, 3303 (1993).
- ¹⁵F. Fuchs, J. Schmitz, H. Obloh, J. D. Ralston, and P. Koidl, *Appl. Phys. Lett.* **64**, 1665 (1994).
- ¹⁶Ch. Gauer, J. Scriba, A. Wixforth, J. P. Kotthaus, C. Nguyen, G. Tuttle, J. H. English, and H. Kroemer, *Semicond. Sci. Technol.* **8**, S137 (1993).
- ¹⁷J. J. Bardeleben, M. O. Manasreh, and C. E. Stutz, in *17th International Conference on Defects in Semiconductors, Gmunden, 1993*, edited by H. Heinrich and W. Jantsch, *Proceedings of Material Science Forum Vols. 143–147* (Trans Tech, Aedermannsdorf, Switzerland, 1994), p. 611.
- ¹⁸J. Schmitz, J. Wagner, H. Obloh, P. Koidl, and J. D. Ralston, *J. Electron. Mater.* (to be published).
- ¹⁹J. Wagner, J. Schmitz, M. Maier, J. D. Ralston, and P. Koidl, in *Proceedings of the Sixth International Conference on Modulated Semiconductor Structures, Garmisch, 1993* [Solid-State Electron. (to be published)].
- ²⁰F. Fuchs, A. Lussion, J. Wagner, and P. Koidl, in *7th International Conference on Fourier Transform Spectroscopy*, edited by D. G. Cameron, *SPIE Proc. Vol. 1145* (SPIE, Bellingham, WA, 1989), p. 323.